Fluorogenic Selective Detection of Zn^{2+} Using a Pyrazole-Ortho-Vanillin Conjugate: Insights from DFT, Molecular Docking, Bioimaging and Anticancer Applications

Malavika S Kumar[a], Sourav Pakrashy[b], Sounik Manna[c], Sujata Maiti Choudhury[c], Bhriguram Das[d], Abhishek Ghosh[e], Asiful H. Seikh[f], Malay Dolai[b*] and Avijit Kumar Das[a*]

[a]Department of Chemistry, Christ University, Hosur Road, Bangalore, Karnataka, 560029 India

Email: avijitkumar.das@christuniversity.in

[b]Department of Chemistry, Prabhat Kumar College, Purba Medinipur 721404, W.B., India

E-mail-dolaimalay@yahoo.in

[c]Biochemistry, Molecular Endocrinology, and Reproductive Physiology Laboratory, Department of Human Physiology, Vidyasagar University, Midnapore721102, W.B., India

[d]Department of Chemistry, Vidyasagar University, Paschim Medinipur 721102, W. B., India

[e] Department of Applied Science, University of Quebec at Chicoutimi, Saguenay, QC, G7H 2B1, Canada

[f]Department of Mechanical Engineering, College of Engineering, King Saud University, Riyadh 11421, Saudi Arabia.

1. General method of UV-vis and fluorescence titration:

By UV-vis method:

For UV-vis titrations, stock solution of the sensor was prepared (c = 5 x 10^{-5} M) in CH_3CN-HEPES buffer (9/1, v/v, 25ºC) at pH 7.4. The solution of the guest interfering analytes like Al^{3+}, Cd^{2+}, Fe^{3+}, Fe^{2+}, Hg^{2+}, Mn^{2+}, Cu^{2+}, Ni^{2+}, Pb^{2+}, Zn^{2+} were also prepared in the order of (c =10^{-5}M). Solutions of various concentrations containing sensor and increasing concentrations of cations were prepared separately. The spectra of these solutions were recorded by means of UV-vis methods.

General procedure for drawing Job plot by UV–vis method:

Stock solution of same concentration of **HMPC** and Zn^{2+} were prepared in the order of ≈ 5.0 × 10^{-5} M in CH_3CN-HEPES buffer (9/1, v/v, 25ºC) at pH 7.4. The absorbance in each case with different *host–guest* ratio but equal in volume was recorded. Job plots were drawn by plotting $\Delta I.X_{host}$ *vs* X_{host} (ΔI = change of intensity of the absorbance spectrum during titration and X_{host} is the mole fraction of the host in each case, respectively).

By fluorescence method:

For fluorescence titrations, stock solution of the sensor (c = 5 × 10^{-5} M) was prepared for the titration of cations in CH_3CN-HEPES buffer (9/1, v/v, 25ºC) at pH 7.4. The solution of the

guest cations in the order of 10^{-5} M were also prepared. Solutions of various concentrations containing sensor and increasing concentrations of cations were prepared separately. The spectra of these solutions were recorded by means of fluorescence methods.

Association constant determination:

The binding constant value of cation Zn^{2+} with the sensor has been determined from the emission intensity data following the modified Benesi–Hildebrand equation, $1/\Delta I = 1/\Delta I$ max + $(1/K[C])$ $(1/\Delta I_{max})$. Here $\Delta I = I\text{-}I_{min}$ and $\Delta I_{max} = I_{max}\text{-}I_{min}$, where Imin, I, and Imax are the emission intensities of sensor considered in the absence of guest, at an intermediate concentration and at a concentration of complete saturation of guest where K is the binding constant and [C] is the guest concentration respectively. From the plot of $(I_{max}\text{-}I_{min})/(I\text{-}I_{min})$ against $[C]^{-1}$ for sensor, the value of K has been determined from the slope. The association constant (K_a) as determined by fluorescence titration method for sensor with Zn^{2+} is found to be 5×10^4 M^{-1} (error < 10%).

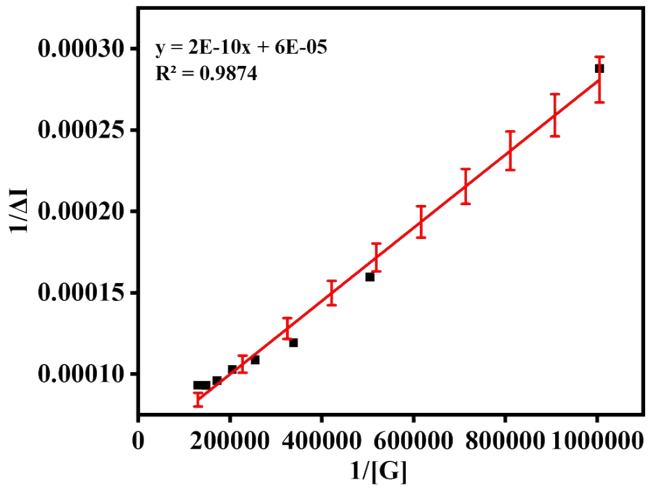

Fig. S1: Benesi–Hildebrand plot from fluorescence titration data of receptor **HMPC** ($c = 5 \times 10^{-5}$ M) with Zn^{2+}.

Determination of fluorescence quantum yield:

Here, the quantum yield φ was measured by using the following equation,

$\varphi_x = \varphi_s (F_x / F_s)(A_s / A_x)(n_x^2/ n_s^2)$

Where,

X & S indicate the unknown and standard solution respectively, φ = quantum yield,

F = area under the emission curve, A = absorbance at the excitation wave length,

n = index of refraction of the solvent. Here φ measurements were performed using anthracene in ethanol as standard [φ = 0.27] (error ~ 10%)

Calculation of the detection limit:

The detection limit DL of **HMPC** for Zn^{2+} was determined from the following equation:

$DL = K^* Sb_1/S$

Where K = 2 or 3 (we take 3 in this case); Sb_1 is the standard deviation of the blank solution; S is the slope of the calibration curve.

From the graph Fig.S2, we get slope = 1593.3, and Sb_1 value is 896.524

Thus using the formula we get the Detection Limit for Zn^{2+} = 1.68 μM

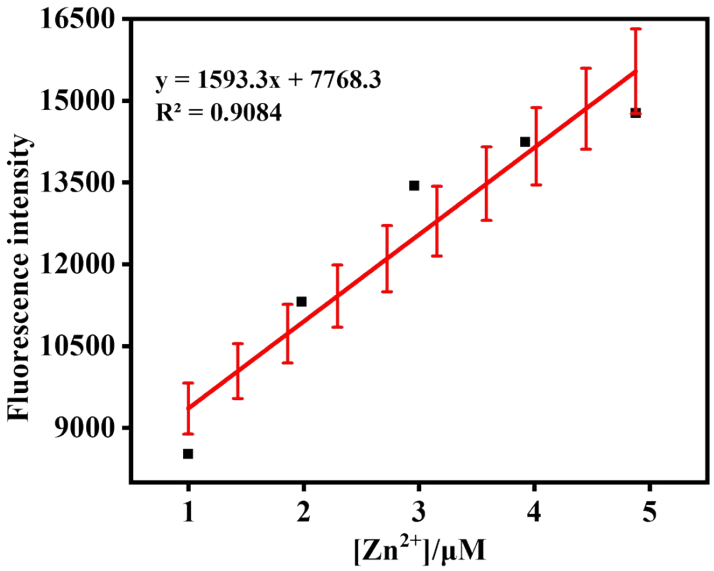

Fig. S2: Changes of fluorescence Intensity of **HMPC** as a function of $[Zn^{2+}]$.

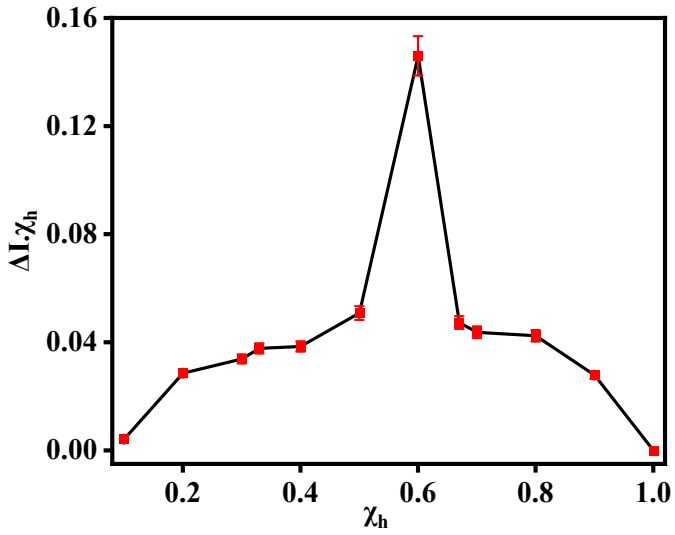

Fig. S3: Job's plot diagram of receptor **HMPC** for Zn^{2+} (where Xh is the mole fraction of host and ΔI indicates the change of the intensity).

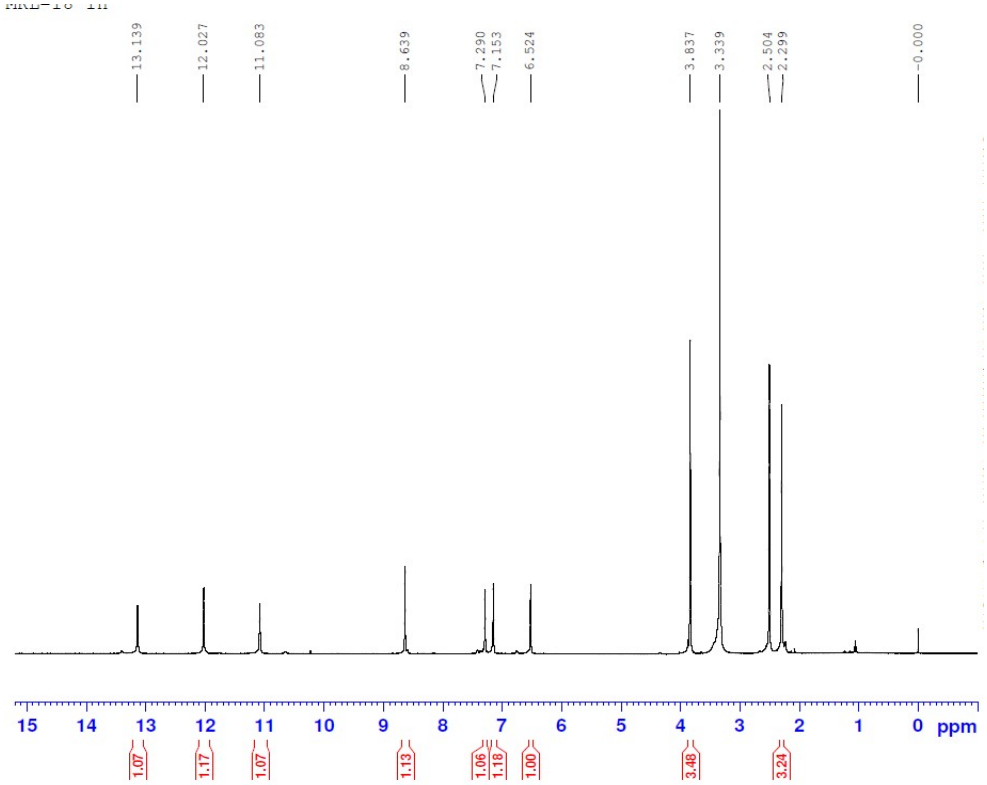

Fig.S4: ^{1}H NMR spectrum of **HMPC**

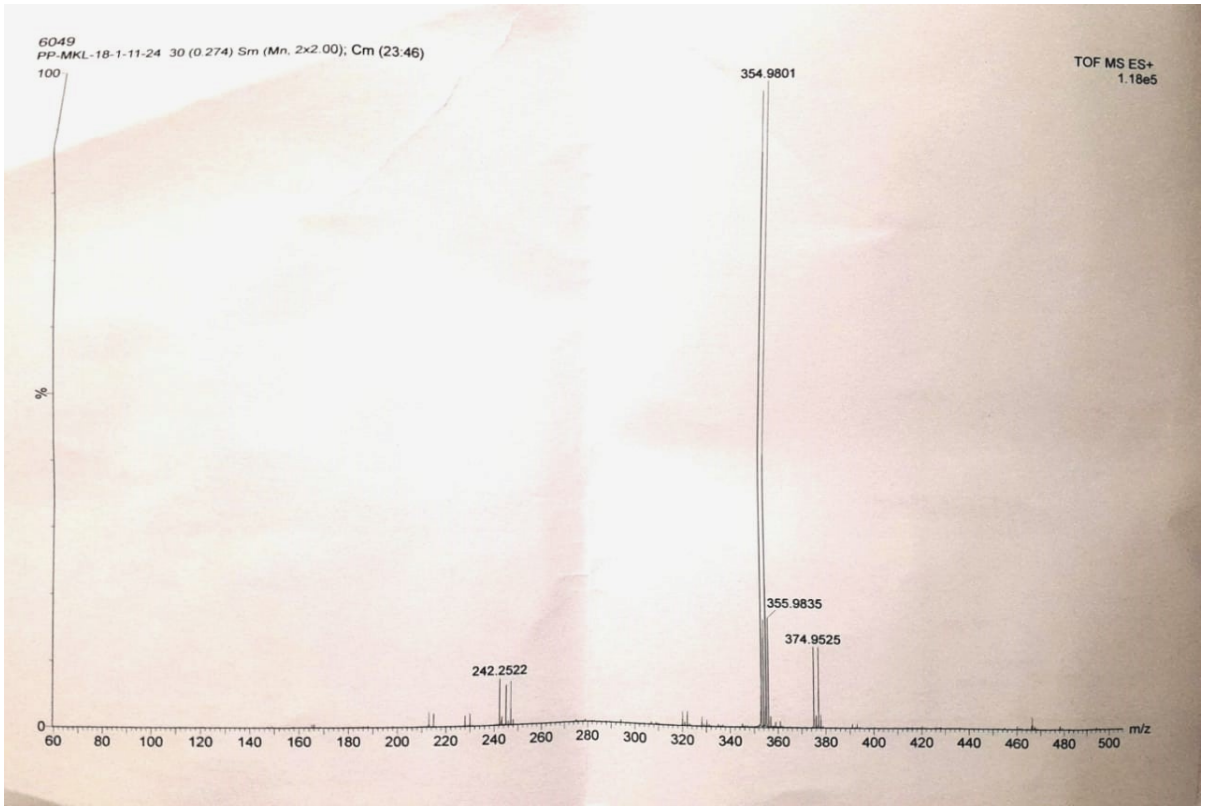

Fig.S5: Mass spectrum of **HMPC**

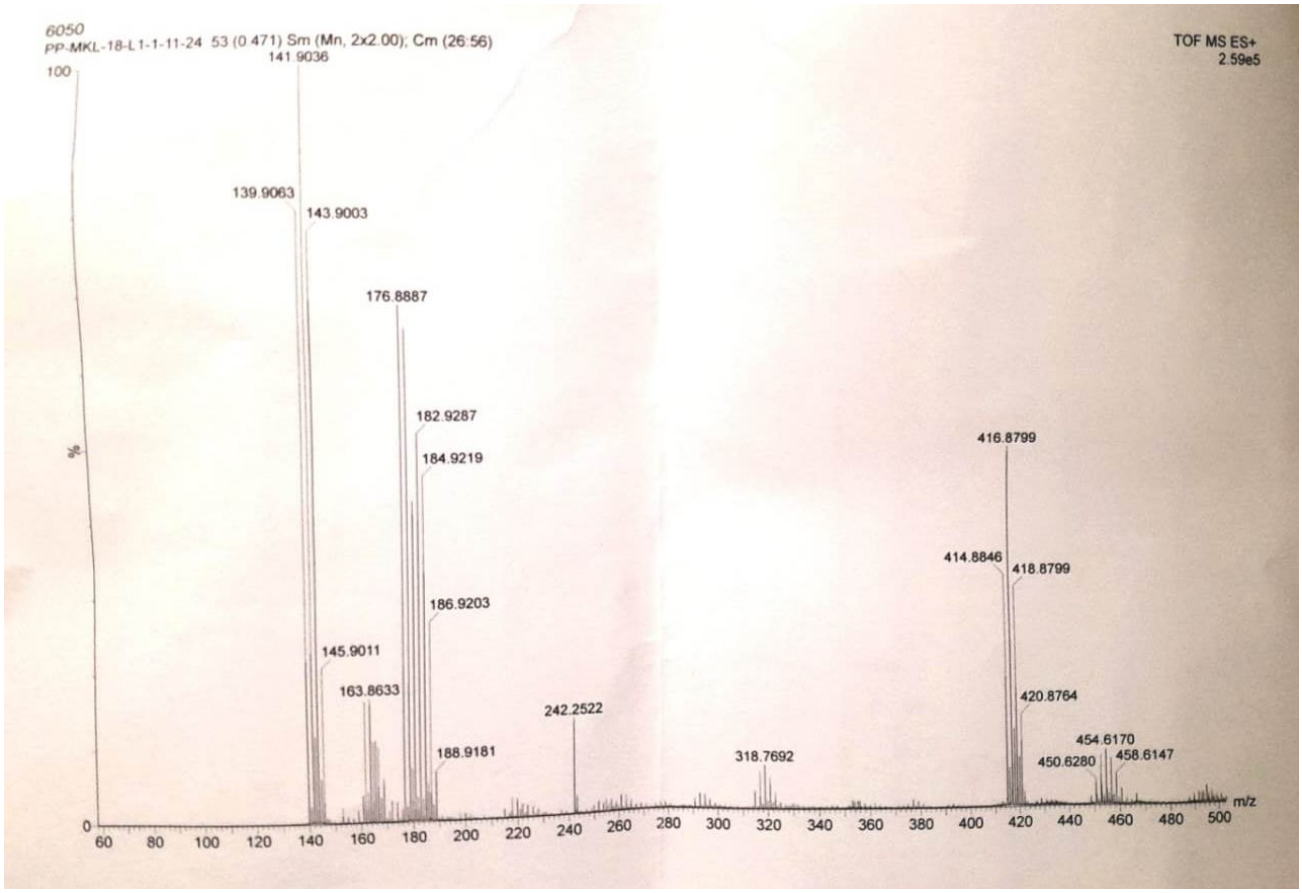

Fig.S6: Mass spectrum of **HMPC** + Zn^{2+}.

2. Experimental conditions:

2.1 Anticancer activity of HMPC and biosensor imaging

Isolation and culture of human lymphocyte cell (HLCs)

Approximately 4 ml of blood was carefully layered onto an equal volume of Histopaque 1077 (Sigma-Aldrich Co. LLC, US) and centrifuged at 2000 rpm for 30 minutes at room temperature. Blood samples (5 ml) were collected from healthy young volunteers according to the Hudson and Hay protocol.[1] After centrifugation, the lymphocyte layer was gently transferred to a fresh tube and washed three times using phosphate-buffered saline (pH 7.4). The isolated human lymphocyte cells (HLCs) were then resuspended in RPMI medium containing 10% fetal bovine serum (FBS) and incubated at 37°C in a CO2 incubator (95% humidity, 5% CO2) for 24 hours to prepare the cells for subsequent cytotoxicity assays.

Cell cytotoxicity study

The cytotoxic effects of the ligand were evaluated through an MTT assay on MCF-7 human breast cancer cells and human lymphocyte cells (HLCs). Cells were plated in 96-well plates and exposed to different concentrations of **HMPC** (ranging from 10 to 100 µg/ml) for 24 hours at 37°C with 5% CO_2. After the treatment period, cells were rinsed and then incubated with MTT solution. This was followed by adding DMSO to dissolve the formazan crystals produced by viable cells. The absorbance at 540 nm was measured using an ELISA plate reader to assess cell viability. A separate experiment was conducted to assess the time-dependent cytotoxicity of **HMPC** at 24-hour and 48-hour intervals. The data were presented as the mean ± SEM based on three separate experiments.[2]

$$\% \text{ cell viability} = (\text{OD of the sample}) / (\text{OD of control}) \times 100$$

2.2 Computational details

Density Functional Theory (DFT)[3] calculations were conducted using the Gaussian 09 (Revision A.02) package, with "Gauss View" utilized for visualizing molecular orbitals. Becke's three-parameter hybrid-exchange functional, the Lee-Yang-Parr expression for nonlocal correlation, and the Vosko-Wilk-Nuair 1980 local correlation functional (B3LYP) were employed in the calculation.[4] Optimization of **HMPC** and single-point energy calculations in the gas phase were performed using the 6-31+(g) basis set. The LanL2dz basis set was used for Zn^{2+} and for H atoms we used 6-31+(g) basis set; for C, N, O, Cl, Zn atoms we employed LanL2DZ as basis set for all the calculations. The calculated electron-density plots for frontier molecular orbitals were prepared by using Gauss View 5.1 software. All the calculations were performed with the Gaussian 09W software package.[5]

2.3 Molecular Docking

The computational docking of the natural product which is protein-ligand binding energy (ΔG) analysis was performed using AutoDock Vina as an extension in UCSF Chimera.[6-7] The protein 4,5-diaryl isoxazole HSP90 chaperone inhibitor - a potential therapeutic agent for the treatment of cancer and Human HDAC8 complexed with SAHA - crystal structure were retrieved from RCSB Protein DataBank (PDB) (http://www.rcsb.org/pdb), PDB-ID 2VCJ and 1T69. The proteins and the ligand were prepared according to our previous published work.[8-15] The charges were assigned as per the ANTECHAMBER algorithm, the energy minimization was done using swiss pdb (SPDBV) viewer, and ligands were adjusted with the Gasteiger algorithm.[16-18] For visualization, Discovery Studio software was used. Ligands

(**HMPC** and SAHA) were drawn in ChemDraw software, converted to SDF in Chem3D software, and finally to PDB using Chimera.

2.4 ADME Prediction

In silico ADME analysis was conducted using SwissADME to investigate physico-chemical properties of the potent hits, such as water solubility, lipophilicity, bio-radar (for orally acceptable molecules), drug likeness, and pharmacokinetics.

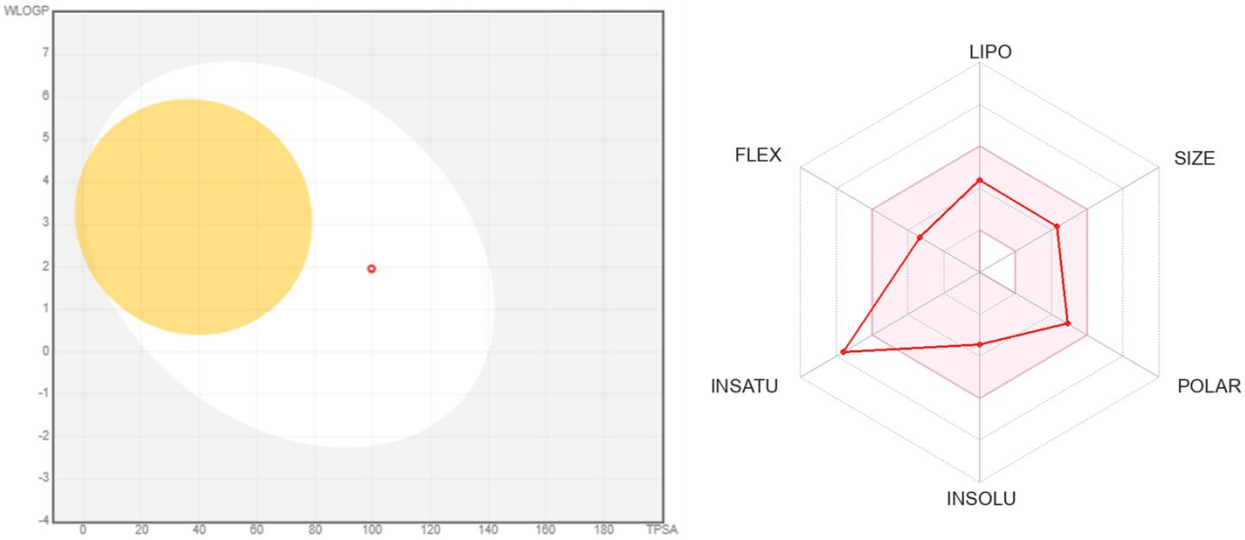

(a) **(b)**

Figure S7: (a) Boiled egg diagram and (b) Bio–radar of **HMPC** for Oral Bio-availability.

Physicochemical Properties		Pharmacokinetics	
Formula	C13H13BrN4O3	**GI absorption**	High
Molecular weight	353.17 g/mol	**BBB permeant**	No
Num. heavy atoms	21	**P-gp substrate**	No
Num. arom. heavy atoms	11	**CYP1A2 inhibitor**	Yes
Fraction Csp3	0.15	**CYP2C19 inhibitor**	No
Num. rotatable bonds	5	**CYP2C9 inhibitor**	No
Num. H-bond acceptors	5	**CYP2D6 inhibitor**	No
Num. H-bond donors	3	**CYP3A4 inhibitor**	No
Molar Refractivity	80.94	**Log K_p (skin permeation)**	-6.91 cm/s
TPSA	99.60 Å²		
Lipophilicity		**Druglikeness**	
Log $P_{o/w}$ (iLOGP)	2.07	**Lipinski**	Yes; 0 violation
Log $P_{o/w}$ (XLOGP3)	2.17	**Ghose**	Yes
Log $P_{o/w}$ (WLOGP)	1.96	**Veber**	Yes
Log $P_{o/w}$ (MLOGP)	0.96	**Egan**	Yes
Log $P_{o/w}$ (SILICOS-IT)	2.69	**Muegge**	Yes
Consensus Log $P_{o/w}$	1.97	**Bioavailability Score**	0.55

Table S1: Results of the ADME property of **HMPC**

Table S2: Comparison table of **HMPC** with the reported similar type of chemosensors

Ligand	Probe type	Detection limit(μM)	References
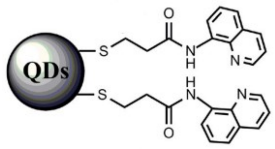	Turn-On	4.5	[19]
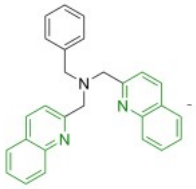	Turn-On	1.2	[20]
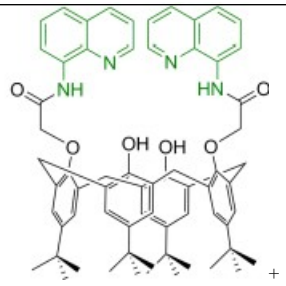	Ratiometric	2.8	[21]
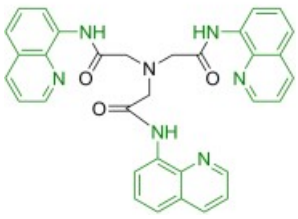	Turn-On	3.2	[22]
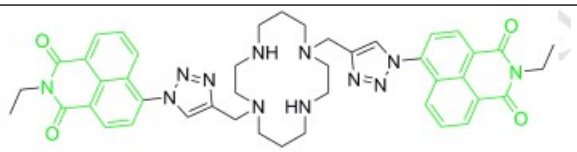	Turn-On	2	[23]
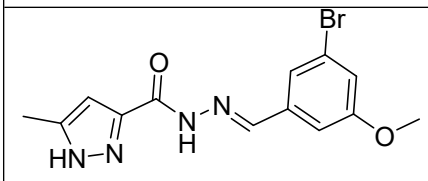	Turn On	1.68	**This work**

3. References

1. L. Hudson and F. C. Hay, Practical immunology, Blackwell Pub, Oxford. (1989).
2. Dey SK, Pradhan A, Roy T, Das S, Chattopadhyay D, Choudhury SM. Biogenic polymer-encapsulated diosgenin nanoparticles: Biodistribution, pharmacokinetics, cellular internalization, and anticancer potential in breast cancer cells and tumor xenograft. Journal of Drug Delivery Science and Technology. 2022 Oct 1;76:103743.
3. R. G. Parr and W. Yang, *Density Functional Theory of Atoms and Molecules*, Oxford University Press, Oxford, 1989.
4. (a) A. D. Becke, *J. Chem. Phys.,* 1993, **98**, 5648. (b) C. Lee , W. Yang and R. G. Parr, *Phys. Rev. B*, 1998, **37**, 785.M. J. Frisch, G. W. Trucks, H. B. Schlegel, G. E. Scuseria, M. A. Robb, J. R. Cheeseman, G. Scalmani, V. Barone, B. Mennucci, G. A. Petersson, H. Nakatsuji, M. Caricato, X. Li, H. P. Hratchian, A. F. Izmaylov, J. Bloino, G. Zheng, J. L. Sonnenberg, M. Hada, M. Ehara, K. Toyota, R. Fukuda, J. Hasegawa, M. Ishida, T. Nakajima, Y. Honda, O. Kitao, H. Nakai, T. Vreven, J. A. Montgomery Jr., J. E. Peralta, F. Ogliaro, M. Bearpark, J. J. Heyd, E. Brothers, K. N. Kudin, V. N. Staroverov, R. Kobayashi, J. Normand, K. Raghavachari, A. Rendell, J. C. Burant, S. S. Iyengar, J. Tomasi, M. Cossi, N. Rega, J. M. Millam, M. Klene, J. E. Knox, J. B. Cross, V. Bakken, C. Adamo, J. Jaramillo, R. Gomperts, R. E. Stratmann, O. Yazyev, A. J. Austin, R. Cammi, C. Pomelli, J. W. Ochterski, R. L. Martin, K. Morokuma, V. G. Zakrzewski, G. A. Voth, P. Salvador, J. J. Dannenberg, S. Dapprich, A. D. Daniels, Ö. Farkas, J. B. Foresman, J. V Ortiz, J. Cioslowski and D. J. Fox, Gaussian Inc., 2009, Wallingford CT.
5. A. Allouche, Software News and Updates Gabedit — A Graphical User Interface for Computational Chemistry Softwares, J. Comput. Chem. 32 (2012) 174–182. https://doi.org/10.1002/jcc.
6. E.F. Pettersen, T.D. Goddard, C.C. Huang, G.S. Couch, D.M. Greenblatt, E.C. Meng, T.E. Ferrin, UCSF Chimera—a visualization system for exploratory research and analysis, J. Comput. Chem. 25 (2004) 1605–1612.
7. S. Pakrashy, P.K. Mandal, J. Nanda Goswami, S.K. Dey, S. Maiti Choudhury, B. Bhattacharya, F. Emmerling, F.A. Alasmary, M. Dolai, Bioinformatics and Network Pharmacology of the First Crystal Structured Clerodin: Anticancer and Antioxidant Potential against Human Breast Carcinoma Cell, ACS Omega. (2022).

8. S. Pakrashy, P.K. Mandal, S.K. Dey, S.M. Choudhury, F.A. Alasmary, A.S. Almalki, M.A. Islam, M. Dolai, Design of a Structurally Novel Multipotent Drug Candidate by the Scaffold Architecture Technique for ACE-II, NSP15, and MproProtein Inhibition: Identification and Isolation of a Natural Product to Prevent the Severity of Future Variants of Covid 19 and a , ACS Omega. 7 (2022) 33408–33422. https://doi.org/10.1021/acsomega.2c04051.
9. S. Misra, S. Pakrashy, S. Paul, P.K. Maurya, P.S. Sardar, A. Bose, A. Majhi, Interaction of a new triazole compound with Serum albumins and Proteolytic enzyme Bromelain by Steady state fluorescence and Molecular docking techniques, (2024).
10. S. Misra, S. Paul, S. Pakrashy, S. Ghosh, S. Naskar, P.K. Maurya, P.S. Sardar, K. Venkateswarlu, A. Bose, A. Majhi, De-Novo drug design of novel 1,2,3–triazole-naphthamide as an inhibitor of SARS-Cov-2 main protease: Synthesis, bioinformatics and biophysical studies, Indian J. Chem. 62 (2023) 1001–1011. https://doi.org/10.56042/ijc.v62i10.1578.
11. M. Dolai, S. Pakrashy, A.K. Ghosh, S. Biswas, S. Konar, F.A. Alasmary, A.S. Almalki, M.A. Islam, Competent DNA binder pentagonal bipyramidal Fe (II) complex executed as a proficient catalyst for primary carbamates production from alcohols and urea, J. Mol. Struct. 1274 (2023) 134584.
12. B. Das, S. Pakrashy, G.C. Das, U. Das, F.A. Alasmary, S.M. Wabaidur, M.A. Islam, M. Dolai, Fashionable Co-operative Sensing of Bivalent Zn2+ and Cd2+ in Attendance of OAc- by Use of Simple Sensor: Exploration of Molecular Logic Gate and Docking Studies, J. Fluoresc. 32 (2022) 1263–1277.
13. S. Pakrashy, A. Majhi, P.K. Maurya, Embelin as an alternative reference standard for Delta-9-Tetrahydrocannibinol, (2024).
14. S. Pakrashy, S. Chakraborty, S. Manna, J. Nanda Goswami, B. Bhattacharya, F. Emmerling, J. Mandal, S. Misra, S. Maiti Choudhury, M.K. Okla, others, Inhibition of Human Colorectal Cancer by a Natural Product 7-Acetylhorminone and Interactions with BSA/HSA: Multispectral Analysis and In Silico and In Vitro Studies, ACS Appl. Bio Mater. (2024).
15. J. Wang, W. Wang, P. a Kollman, D. a Case, Antechamber, An Accessory Software Package For Molecular Mechanical Calculations, J. Am. Chem. Soc. 222 (2001) U403.
16. N. Guex, M.C. Peitsch, SWISS-MODEL and the Swiss-PdbViewer: An environment for comparative protein modeling, Electrophoresis. 18 (1997) 2714–2723. https://doi.org/10.1002/elps.1150181505.

17. J. Gasteiger, C. Jochum, An Algorithm for the Perception of Synthetically Important Rings, J. Chem. Inf. Comput. Sci. 19 (1979) 43–48. https://doi.org/10.1021/ci60017a011.
18. A. Daina, O. Michielin, V. Zoete, SwissADME: a free web tool to evaluate pharmacokinetics, drug-likeness and medicinal chemistry friendliness of small molecules, Sci. Rep. 7 (2017) 42717.
19. Z. Liu, G. Li, Q. Ma, L. Liu and X. Su, Microchim. Acta, 2014, 181, 1385.
20. Kim, H. Kang, J. Kim, KB. Song, EJ. Kim, C. A highly selective quinoline-based fluorescent sensor for Zn(II). Spectrochim Acta A 2014; 118: 883–887
21. Mummidivarapu, VVS. Tabbasum, K. Chinta, JP. Rao, CP. 1,3-Di-amidoquinoline conjugate of calix[4]arene (L) as a ratiometric and colorimetric sensor for Zn2+: spectroscopy, microscopy and computational studies. Dalton Trans 2012; 41: 1671–1674.
22. Goswami, S. Das, AK. Aich, K. Manna, A. Maity, S. Khanra, K. Bhattacharyy, N. Ratiometric and absolute water-soluble fluorescent tripodal zinc sensor and its application in killing human lung cancer cells. Analyst 2013; 138: 4593–4598
23. Tamanini, E. Flavin, K. Motevalli, M. Piperno, S. Gheber, LA. Todd, MH. Watkinson, M. Cyclam-based “clickates”: homogeneous and heterogeneous fluorescent sensors for Zn(II). Inorg Chem 2010; 49: 3789–3800.